Vol. 732: 149–166, 2024
https://doi.org/10.3354/meps14551

MARINE ECOLOGY PROGRESS SERIES
Mar Ecol Prog Ser

Published March 20

Early growth and environmental conditions control partial migration of an estuarine-dependent fish

Kohma Arai[1,2,*], Jessica E. Best[3], Caitlin A. Craig[4], Vyacheslav Lyubchich[1], Nathaniel R. Miller[5], David H. Secor[1]

[1]Chesapeake Biological Laboratory, University of Maryland Center for Environmental Science, Solomons, MD 20688, USA
[2]Center for Watershed Sciences, University of California, Davis, Davis, CA 95616, USA
[3]New York State Department of Environmental Conservation, Division of Marine Resources, Department of Natural Resources, Cornell University, New Paltz, NY 12561, USA
[4]New York State Department of Environmental Conservation, Division of Marine Resources, Kings Park, NY 11754, USA
[5]Jackson School of Geosciences, The University of Texas at Austin, Austin, TX 78712, USA

ABSTRACT: Partial migration is a widespread phenomenon in animals, whereby multiple groups follow different migration behaviors (i.e. contingents) within a single population. Fishes exhibit particularly high diversity in their early dispersal behaviors; however, whether these represent conditional partial migration behaviors remains unclear. We combined otolith microstructure and chemistry to assess the influence of early life conditions and environmental drivers on juvenile-stage partial migration of anadromous striped bass *Morone saxatilis* in the Hudson River (USA) in 2 consecutive years with contrasting hydrologic conditions. Time series clustering on otolith strontium (Sr) and barium (Ba) profiles revealed 4 dominant early migration contingents in both years: freshwater residents, oligohaline migrants, small mesohaline migrants, and large mesohaline migrants. In both years, juvenile partial migration appeared to be a conditional strategy linked to a growth-mediated threshold. The propensity to migrate early was related to slower larval growth, whereas freshwater residency and delayed migration were associated with faster larval growth. Differences in hatch dates may have indirectly affected migration contingents by exposing larvae to varying environmental conditions. In the dry year, dispersal timing to mesohaline habitats coincided with high freshwater flow and tidal currents, but not so in the higher-flow year. Recruitment to coastal nurseries outside the Hudson River occurred primarily during the juvenile phase. Early migration contingents could carry over to population dynamics, whereby diverse estuarine nursery habitats contribute differently to recruitment.

KEY WORDS: Partial migration · Estuary · Otolith chemistry · Striped bass · *Morone saxatilis* · Hudson River

1. INTRODUCTION

Partial migration is a common attribute observed for a range of animals, in which a single population contains multiple groups that follow different migration trajectories (i.e. contingents) (Lundberg 1988, Chapman et al. 2011, Berg et al. 2019, Menz et al. 2019). The most traditional view is the coexistence of individuals that remain in a single habitat (i.e. residents) and those that migrate between multiple habitats (i.e. migrants). Partial migration can alter the food web and community structure (Peller et al. 2023), and regulate population structure and species persistence (Kerr et al. 2010), all of which can have important ecological, evolutionary, and conservation consequences (Schindler et al. 2010, Secor 2015). Yet,

*Corresponding author: kharai@ucdavis.edu

remarkably little attention has been given to how partial migration overlays complex life cycles — life cycles that entail abrupt changes in body form and function from one life stage to the next and that are widespread among fishes (Secor 2015).

Partial migration in fishes has long been recognized among salmonid species (Jonsson & Jonsson 1993, Dodson et al. 2013), and may be prevalent among fishes in general (Kerr et al. 2009, Chapman et al. 2012, Secor 2015). Discrete migration contingents have been shown to arise from a conditional response early in life in which intrinsic factors such as early development interact with extrinsic factors like environmental conditions, density-dependence, and predation risk (Lundberg 1988, Chapman et al. 2012, Secor 2015). This conditional response on whether to migrate or to remain resident is dependent upon thresholds related to early life conditions such as body size and growth (Pulido 2011, Dodson et al. 2013). Accelerated early growth has been associated with residency in Arctic charr *Salvelinus alpinus*, Atlantic salmon *Salmo salar*, and brown trout *Salmo trutta* (Nordeng 1983, Aubin-Horth & Dodson 2004, Olsson et al. 2006), but in other populations, the opposite has been shown, with higher growth favoring migration (Metcalfe et al. 1989, Forseth et al. 1999, Rikardsen & Elliott 2000). Conditional responses could be multi-modal, as in the case of Atlantic salmon, where (1) the fastest-growing juveniles mature early and remain resident (i.e. residents), (2) the intermediate-growing juveniles migrate early after brief residency (i.e. early migrants), and (3) the slowest-growing juveniles migrate later in life after remaining resident for a longer period (i.e. late migrants) (Secor 2015). Outside of salmonids, the estuarine-dependent white perch *Morone americana* forms resident and migratory contingents linked to early growth, with faster-growing individuals adopting a resident life cycle in freshwater habitats (Kraus & Secor 2004, Kerr & Secor 2010, Gallagher et al. 2018). Yet, the slower-growing migratory contingent shows compensatory growth, wherein juveniles accelerate their post-dispersal growth by taking advantage of the more productive brackish-water environment (Kerr & Secor 2009, Gallagher et al. 2018).

Partial migration can be considered a series of ecological carryover effects, in which conditions experienced during one life stage affect the behavior of subsequent life stages (Pechenik 2006, O'Connor et al. 2014). Hatch dates and early-life environmental conditions (e.g. temperature, food availability) can directly influence early growth, which in turn determines whether an individual adopts a particular migration behavior (Kraus & Secor 2004, Kerr & Secor 2010, Gallagher et al. 2018). Hatch date could also be the proximate driver of migration propensity through intraspecific competition, with early-hatched cohorts pre-occupying favorable habitats and forcing later-hatched, smaller individuals to seek alternate habitats (MacCall 1990, Chapman et al. 2012). As such, inter-annual fluctuations in weather conditions and larval production cause annual variations in juvenile contingent proportions and nursery habitat use that carry over to influence adult life history, which ultimately contributes to population-level stability and resilience (Kraus & Secor 2004, Kerr et al. 2010).

The potential causes and consequences of partial migration during the early life stage were investigated for the Hudson River (HR) population of striped bass *Morone saxatilis*, an estuarine-dependent fish that supports important commercial and recreational fisheries in US Atlantic waters (NEFSC 2019). Striped bass are anadromous, whereby most adults spend the majority of their lifetime in coastal waters showing diverse oceanic migrations (Zlokovitz et al. 2003, Secor & Piccoli 2007, Gahagan et al. 2015), but migrate into fresh tidal regions to spawn in the spring (Secor & Houde 1995, Pan et al. 2023). Semi-buoyant eggs and pelagic larvae are redistributed by freshwater flow and tidal currents, but are generally retained above the salt front (Boreman & Klauda 1988, Dovel 1992, Secor et al. 2020). Following metamorphosis (at ca. 15 mm total length [TL]; Mansueti 1958), juveniles occur throughout a wide range of salinity in the HR (Dovel 1992).

Striped bass juveniles exhibit partial migration in the Albemarle Sound (Mohan et al. 2015), Chesapeake Bay (Conroy et al. 2015), and St. Lawrence Estuary (Morissette et al. 2016, Vanalderweireldt et al. 2019), whereby a portion of juveniles remains in natal freshwater or oligohaline habitats, while others migrate downstream into higher-salinity habitats. Slower early growth was associated with a propensity to migrate, and the timing of dispersal was related to a high-flow event in a Chesapeake Bay population (Conroy et al. 2015). We hypothesized that HR striped bass might similarly exhibit juvenile migrations that are conditionally influenced by larval growth and facultatively controlled by flow. In addition to the principal nursery region within the HR, juveniles frequently occur outside the HR, in the nearby western Long Island Sound (WLIS) region (Fig. 1), which may provide important contributions to the HR adult population (Dovel 1992, Dunning et al. 2009). Freshwater and tidal flow can transport lar-

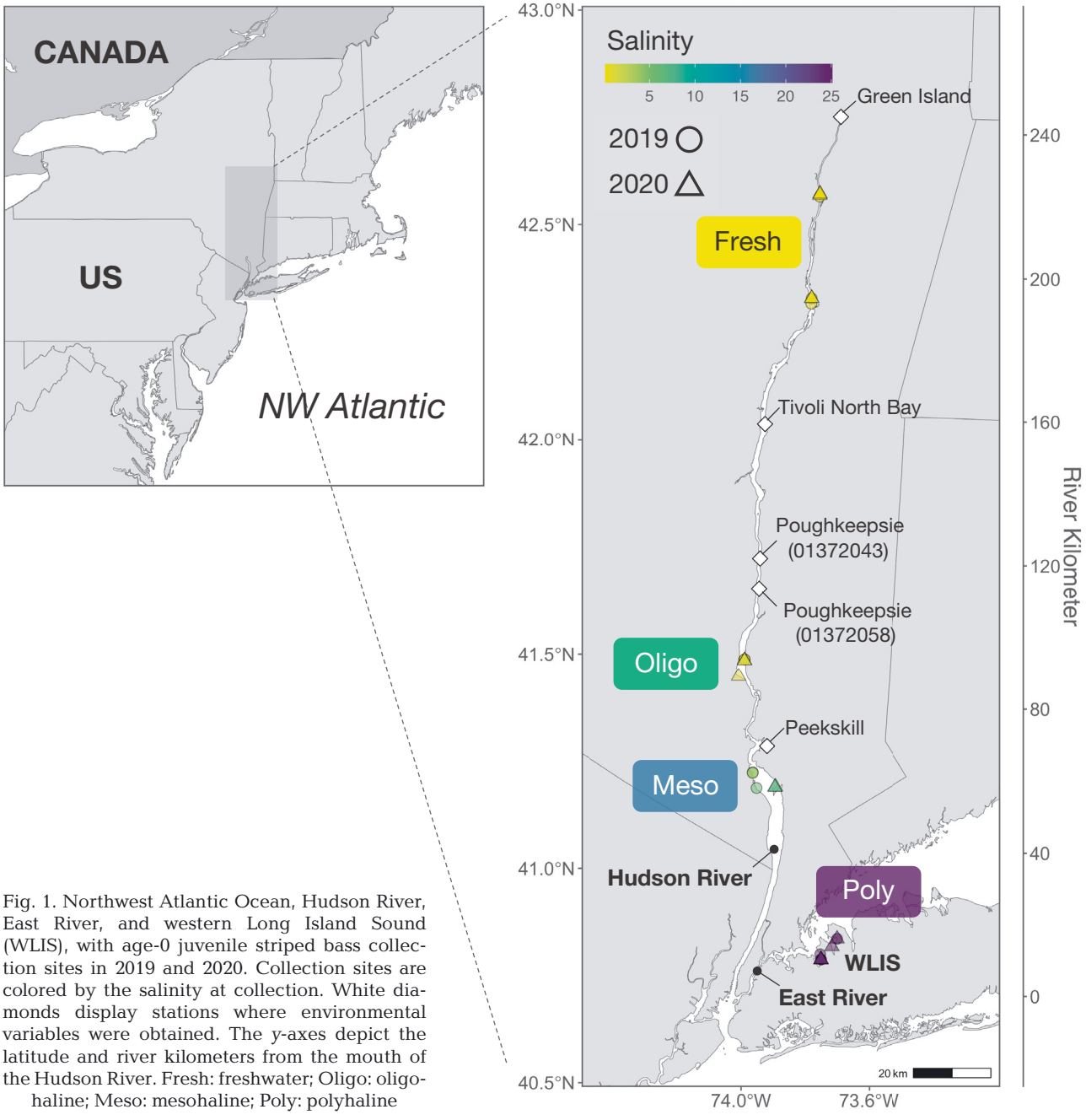

Fig. 1. Northwest Atlantic Ocean, Hudson River, East River, and western Long Island Sound (WLIS), with age-0 juvenile striped bass collection sites in 2019 and 2020. Collection sites are colored by the salinity at collection. White diamonds display stations where environmental variables were obtained. The *y*-axes depict the latitude and river kilometers from the mouth of the Hudson River. Fresh: freshwater; Oligo: oligohaline; Meso: mesohaline; Poly: polyhaline

vae from the HR to WLIS via the highly channelized East River (Dunning et al. 2009), although dispersal dynamics to WLIS nurseries remain highly uncertain. Understanding juvenile striped bass partial migration at fine spatiotemporal scales, as well as the potential drivers that regulate these behaviors, would be beneficial not only for conservation and management of this important species, but also for gaining a better understanding of how partial migration dynamics shape complex life cycles in fishes in general.

Here, we used otolith microstructure and microchemistry to understand how early life conditions and environmental drivers are related to the partial migration of juvenile HR striped bass in 2 consecutive years (2019 and 2020) with contrasting hydrologic conditions and age-0 juvenile recruitment levels (Fig. S1 in the Supplement at www.int-res.com/articles/suppl/m732p149_supp.pdf). Fine-scale larval and juvenile movement patterns were reconstructed by combining otolith microstructure and chemical analyses with

time series clustering and machine learning algorithms. Because otoliths are metabolically inert and permanently record daily growth and ambient environmental conditions, elements such as Sr and Ba have been used extensively to understand diadromous fish migrations across salinity gradients at high resolution (Elsdon et al. 2008, Walther & Limburg 2012, Walther 2019). We hypothesized that (1) HR striped bass juveniles would exhibit distinct early migration contingents; (2) differences in larval growth would lead to distinct migration contingents; (3) migration contingents would be indirectly influenced by hatch dates and early-life environmental conditions through the effects of these variables on larval growth; (4) dispersal timing would be associated with environmental drivers; and (5) migrants would compensate for their slower growth by enhancing post-dispersal juvenile growth in productive brackish habitats (Fig. 2).

2. MATERIALS AND METHODS

2.1. Sample collection

Age-0 striped bass juveniles were collected during the New York State Department of Environmental Conservation annual young-of-year survey from July to November 2019 (n = 193), and from June to November 2020 (n = 448). Collections took place in freshwater (salinity <0.4 ppt), oligohaline (0.4–3 ppt), and mesohaline (3–18 ppt) habitats in the HR, and in polyhaline (>18 ppt) habitats outside the HR estuary in the WLIS (Fig. 1). A 30.5 m × 3.1 m (0.48 cm mesh) beach seine was used in the HR, and a 61.5 m × 3.1 m (0.64 cm mesh) beach seine, with a 7.6 m × 3.7 m (0.48 cm mesh) bunt area, was used in the WLIS. TL was measured to the nearest 1 mm, and a sagittal otolith was extracted from all samples. Otoliths for microstructure and microchemistry were subsampled

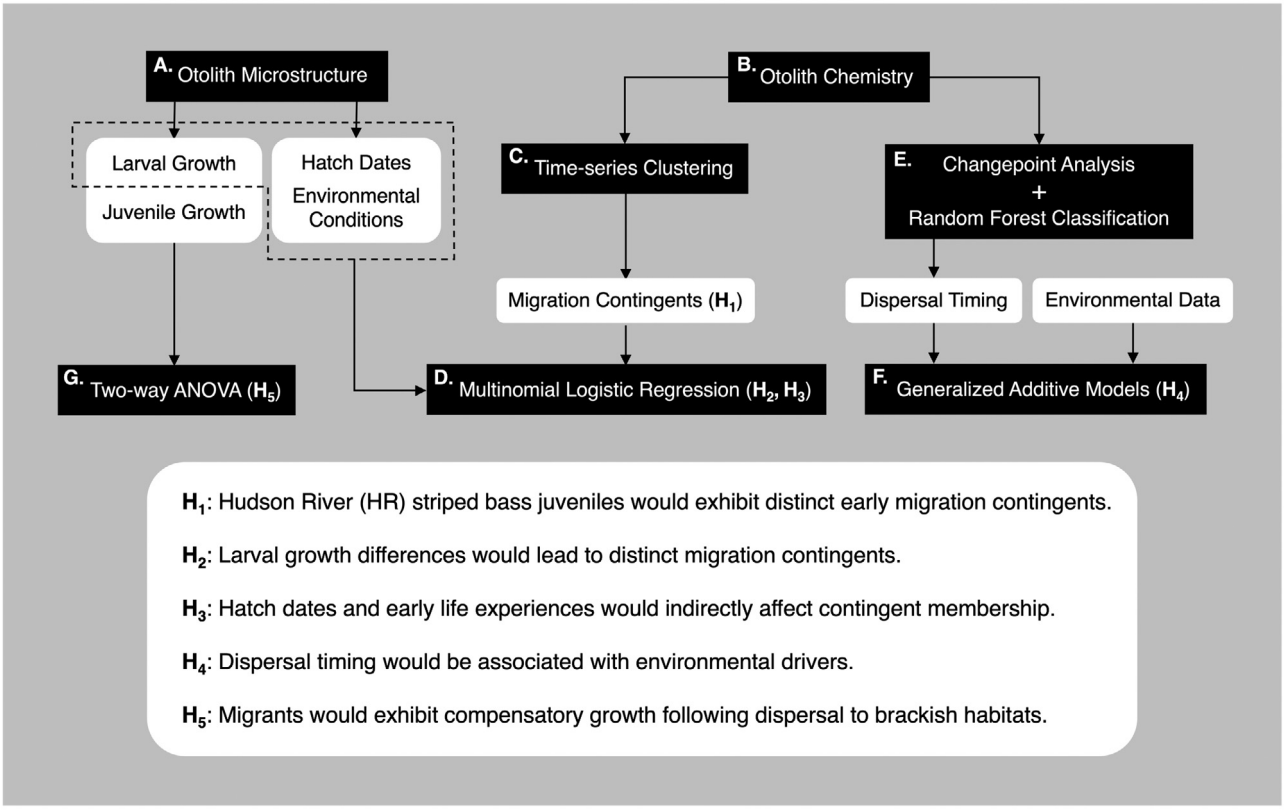

Fig. 2. Steps for otolith microstructure, chemistry, statistical analyses, and testing of related hypotheses (H_1–H_5) for Hudson River (HR) juvenile striped bass. (A) Otolith microstructure analysis to estimate larval and juvenile growth, hatch dates, and environmental conditions (water temperature, flow, and chlorophyll *a*) experienced during the first 30 d of life for each individual. (B) Otolith microchemistry to reconstruct early dispersal history for juvenile striped bass. (C) Time-series clustering on otolith chemistry to identify distinct early migration contingents of juveniles. (D) Multinomial logistic regression to assess the effect of larval growth, hatch dates, and early life history experiences on migration contingents. (E) Time-series changepoint analysis with random forest classification to detect the size and age at dispersal to brackish habitats. (F) Generalized additive models to assess the influence of environmental conditions on dispersal timing. (G) Two-way ANOVA to detect differences in larval and juvenile growth to test the compensatory growth hypothesis following dispersal

from months after June assuming that juveniles would have completed their initial dispersal and settled in their nurseries by this time (Dovel 1992, Conroy et al. 2015), and included subsamples from July to October 2019 (n = 69) and from July to August 2020 (n = 62). To the extent possible, subsamples were evenly selected across freshwater, oligohaline, mesohaline, and polyhaline regions; within regions, individuals were drawn randomly to obtain a representative size distribution (Table S1). Subsamples from all regions, aside from polyhaline habitats, were selected from July and August. For polyhaline habitats in the WLIS, the small sample size required us to select samples from July to October.

2.2. Otolith microstructure

Hatch dates and early growth were estimated through otolith microstructure analysis (step A in Fig. 2). Following Secor et al. (1991), otoliths were embedded and sectioned transversely. Otolith sections were subsequently polished using 320-, 600-, and 1200-grit materials until the primordium was visible. Sections were then buffed on a wet microcloth with 0.3 µm alumina powder to remove pits and abrasions. Because the daily deposition of microstructural increments in sagittal otoliths has been validated for juvenile striped bass (Secor & Dean 1989), increments were enumerated from the primordium to the otolith edge to determine daily age. A second read on a subset of samples (n = 30) detected no ageing bias and high ageing precision (see Text S1, Fig. S2). The following equation from Houde & Morin (1990) was used to adjust the initial age estimate (a_{initial}) for the effects of temperature on the formation of the first daily increment in striped bass otoliths ($a_{\text{corrected}}$):

$$a_{\text{corrected}} = a_{\text{initial}} + (11.56 - 0.45 \times T) \quad (1)$$

where T is the mean daily water temperature (°C) on the preliminary hatch date calculated using a_{initial}. Age adjustments were small and ranged from 0 to 4 d. Water temperature data were obtained from the United States Geological Survey (USGS) monitoring station below Poughkeepsie, NY (site: 01372058), in 2019, and near Poughkeepsie (site: 01372043; Fig. 1) in 2020, because single-site data were not available for both years.

The otolith radius (OR, µm) along the ventral transverse axis from the primordium to a given daily increment was measured using Infinity Analyze and Capture (Teledyne Lumenera software). The biological intercept method was then used to back-calculate the TL (mm) of an individual at any given age by the following equation (Campana 1990):

$$TL_a = TL_c + \frac{(OR_a - OR_c) \times (TL_c - TL_i)}{(OR_c - OR_i)} \quad (2)$$

where subscripts i, a, and c correspond to initial, at-age, and at-capture values, respectively, of OR and TL. Values of 23.9 µm and 6.1 mm were used as inputs for OR_i and TL_i, respectively (Conroy et al. 2015). Back-calculated size-at-age was used to estimate specific growth rate (SGR, % d^{-1}) during the larval (ages 0 to 30 d) and early juvenile stages (ages 30 to 50 d) (Mansueti 1958) using the following equation:

$$SGR = \frac{\log(TL_f) - \log(TL_i)}{d} \times 100 \quad (3)$$

where TL_f and TL_i are final and initial total lengths, respectively, and d is the age between those 2 lengths. We used a theoretical size-at-hatch (i.e. age 0) of 3.81 mm for larval growth estimates (Conroy et al. 2015).

2.3. Otolith microchemistry

Early dispersal history for each age-0 juvenile was reconstructed using otolith microchemistry (step B in Fig. 2). Elemental concentrations in otoliths were measured using an Elemental Scientific NWR193 excimer laser ablation (LA) system (193 nm, 4 ns pulse width) coupled to an Agilent 7500ce inductively coupled plasma mass spectrometer (ICP-MS) at the University of Texas at Austin. All otoliths and standards processed on the LA-ICP-MS were loaded into a large-format cell with fast washout times (<1 s). Following pre-ablation (50 µm diameter spot, 50 µm s^{-1} scan rate, 3.9 J cm^{-2} fluence) to remove shallow surface contaminants of the otolith section, a laser transect scan was performed from the primordium (start of life) along the longest growth axis to the otolith edge (end of life) with a 25 µm diameter spot, 5 µm s^{-1} scan rate, 2.77 ± 0.06 J cm^{-2} fluence, 20 Hz repetition rate, and carrier gas flows of 0.8 l min^{-1} for argon and helium. All elements (^{24}Mg, ^{44}Ca, ^{55}Mn, ^{88}Sr, ^{138}Ba) were measured on the LA-ICP-MS system with 10 ms integration times. Measured intensities were converted to elemental concentrations (ppm) with Iolite software (Paton et al. 2011), using ^{43}Ca as the internal standard (known elemental concentration) and a Ca index concentration value of 38.3 wt% for juvenile striped bass otoliths (unknown elemental concentration). USGS MACS-3 (synthetic aragonite) was used as the primary calibration standard, and NIST 612 and ECRM-752-NP were used

as external reference standards. The grand average of secondary standard recovery fractions for all elements was typically within 5% of reference values (http://georem.mpch-mainz.gwdg.de).

2.4. Statistical analysis

Elemental concentration profiles from the otolith core to the edge were smoothed by consecutive moving median and average filters using a 7-point boxcar width (5 µm equivalent distance) to remove high-frequency outliers. Multivariate time-series clustering using dynamic time warping (DTW) was employed to identify distinct early migration contingents of age-0 juveniles based on the shapes of otolith elemental profiles (Aghabozorgi et al. 2015, Hegg & Kennedy 2021) (step C in Fig. 2). The DTW algorithm clusters time series that are similar in shape but are offset in time, which would otherwise bias traditional Euclidean distance-based clustering (Aghabozorgi et al. 2015). The algorithm reports the cost of 'warping' the temporal dimension to match 2 time series by iteratively matching each point in the 2 time series in a one-to-multiple approach. In this way, otolith elemental profiles that are similar in shape but vary temporally are clustered together as a unique migration contingent. Clustering was performed jointly on Sr and Ba profiles with the R package 'dtwclust' (Sardá-Espinosa 2019) using agglomerative hierarchical clustering with Ward's distance. The 'dtw_basic' function was used for DTW implementation. A Sakoe-Chiba window of 1.5% was used to restrict the warping path between 2 time series. All elemental concentration time series were standardized to *z*-scores before analysis. The dendrogram was cut (i.e. the number of clusters) at the location that produced interpretable distinct migration contingents with a high Silhouette index (Rousseeuw 1987), while also maintaining a minimum ($n > 10$) within-cluster sample size for subsequent analysis. In addition, otolith chemistry near the core region was assessed to test whether distinct migration contingents were associated with different spawning locations (see Text S2, Fig. S3).

Partial migration is likely shaped by multiple factors, including hatch dates and early life environmental conditions, rather than just the conditional response to larval growth (step D in Fig. 2). Thus, in addition to larval growth, we explored the environmental conditions and food availability experienced by age-0 juveniles during their first 30 d of life. The mean water temperature, river flow, and chlorophyll *a* (chl *a*) concentration experienced by each individual during its first 30 d of life were calculated. Here, chl *a* concentrations were used as a surrogate for estuarine production and trophic resources, as zooplankton prey (data unavailable) are expected to be positively associated with primary production (Pace et al. 1998). Data on daily water temperature, river flow, and chl *a* concentration were acquired from the USGS Poughkeepsie monitoring station (site: 01372058 [2019], 01372043 [2020]), USGS Green Island monitoring station (site: 01358000), and the National Estuarine Research Reserve System (NERRS) at Tivoli North Bay, respectively (Fig. 1). These metrics were calculated independently of habitat use determined by otolith chemistry, and thus represented differences in experienced environmental conditions due to hatch date differences.

To examine the effect of larval growth, hatch dates, and early life experiences on migration contingents, a multinomial logistic regression analysis was conducted using the R package 'nnet' (Venables & Ripley 2002). The migration contingent was modeled as a categorical response variable, and larval growth, hatch dates, and experienced environmental conditions (i.e. mean water temperature, river flow, and chl *a*) were included as continuous predictor variables. Given the strong collinearity ($r > |0.6|$) among hatch dates and experienced environmental conditions, we initially conducted a principal component analysis on these correlated variables and included the first principal component (PC1, >90% variance explained) as a continuous predictor in the model (Fig. S4). The relationship between the log-odds of belonging to any migration contingent *j* relative to a reference category (1) and continuous predictors was modeled as follows:

$$\ln\left(\frac{P_j}{P_1}\right) = \beta_{0j} + \beta_1(\text{Larval Growth}_j) + \beta_2(\text{PC1}_j) \quad (4)$$

where Larval Growth_j and PC1_j (i.e. first principal component) are continuous predictors.

Separate models were fitted to 2019 and 2020 data, and the best model was selected by comparing Akaike's information criterion corrected for small sample sizes (AICc). Predicted probabilities of migration contingents associated with each predictor were visualized using the R packages 'emmeans' (Lenth et al. 2022) and 'ggeffects' (Lüdecke 2018). The effect of hatch dates and early life experiences on larval growth is shown in Text S3. Univariate comparisons of hatch dates and early life experiences across migration contingents and years are shown in Text S4 (and see Fig. S5).

The hypothesis related to dispersal timing (step E in Fig. 2) was assessed using time-series changepoint

analysis with the pruned exact linear time (PELT) algorithm in the R package 'changepoint' (Killick & Eckley 2014), which detected major concentration shifts within the individual otolith Sr transect. AIC was used as the penalty value for minimizing the cost function to detect the number and location of changepoints. The PELT algorithm detected multiple shifts in mean and variance in Sr concentration for each fish, resulting in multiple stable otolith signature segments for a given transect. For each stable segment, we calculated the mean concentration of 4 elements (i.e. Mg, Mn, Sr, Ba); then, each segment was assigned to 1 of 4 habitats (freshwater, oligohaline, mesohaline, or polyhaline) using a random forest (RF) algorithm in the R package 'ranger' (Wright & Ziegler 2017). RF is a machine learning algorithm that demonstrates high performance in classification and regression tasks by constructing and aggregating predictions from a large number of trees, each recursively partitioning the input data into homogeneous subsets (Breiman 2001, Hastie et al. 2009). Mean elemental concentrations of the recently formed otolith edge, corresponding to the last 20 µm of the laser transect, were used as the reference baseline for habitat assignment, assuming that it reflects the habitat from which the sample was collected (Fig. S6A) (Morissette et al. 2016, 2021, Vanalderweireldt et al. 2019). All samples were used to establish the reference baseline, except for recent migrants, whose otolith chemistry was not likely to reflect the ambient environmental conditions of their collection sites (see Section 3). Hyperparameter tuning of the RF classifier was conducted through a grid search method on 10 cross-validation folds to find the optimal hyperparameters (mtry = 2, minimal node size = 1, number of trees = 1000). The accuracy of the RF classifier was further assessed through 10-fold cross-validation. For each fish, detected changepoints and assigned habitats were visually inspected, and erroneous changepoints and assignments associated with unstable means were manually removed. The changepoint detected near the core region was also removed given that the elemental signature near the core may be maternally derived (Kalish 1990, Volk et al. 2000, Hegg et al. 2019). We defined the size and age at dispersal to brackish habitats as the first point at which an individual transitioned from freshwater to brackish-water habitats (i.e. oligohaline, mesohaline, or polyhaline).

We further evaluated the size and age of WLIS entrance for fish that were collected in polyhaline habitats in WLIS. Given the distinct otolith Ba signature in WLIS habitats (Fig. S6B), a similar changepoint analysis with the PELT algorithm was performed on otolith Ba transects, using only the transects past the point of initial dispersal to brackish-water habitats. Mean stable segments were further assigned to a specific habitat using RF to detect WLIS entry. We defined WLIS entry as the point at which the fish entered polyhaline habitats and demonstrated subsequent usage of polyhaline habitats after entry. To assess the effect of the initial dispersal size to brackish habitats on the number of days spent in brackish water before entering WLIS, a generalized linear model with a negative binomial distribution and a log-link function was used in the R package 'MASS' (Venables & Ripley 2002).

The effect of environmental conditions on dispersal timing was assessed using nonlinear regression models (step F in Fig. 2). Because the shift in otolith Sr concentration for oligohaline migrants was less apparent (see Section 3) and could potentially bias estimates of dispersal date, this analysis was limited to fish that dispersed to mesohaline and polyhaline habitats (2019: n = 30, 2020: n = 26). The number of fish dispersed on a given day was estimated from the dispersal date of each fish, then smoothed using a 5 d centered moving average window to account for ageing error and the potential lag effect of elemental uptake into otoliths (Elsdon & Gillanders 2005). The smoothed daily number of fish dispersed was then compared to the daily mean water temperature, river flow, and tidal amplitude data acquired from the USGS Poughkeepsie monitoring station (site: 01372058 [2019], 01372043 [2020]), USGS Green Island monitoring station (site: 01358000), and the NOAA Tide and Currents Peekskill monitoring station (site: 8518949), respectively. We employed a generalized additive mixed model (GAMM) in the R package 'mgcv' (Wood 2017) to assess the influence of environmental conditions on dispersal timing. GAMMs can account for temporal autocorrelation of residuals and allow non-linear relationships between predictors and response variables (Wood 2017). The smoothed number of fish dispersed on a given day t, Y_t, was specified using a gamma distribution as the response variable, modeled as a combination of additive smooth terms through a log link function defined as:

$$Y_t \sim \text{Gamma}(\mu_t) \tag{5}$$

$$\ln(\mu_t) = \beta_0 + s(\text{Temperature}_t) + s(\text{Flow}_t) + s(\text{Tide}_t) + \beta_1 \text{Year}_t + \varepsilon_t \tag{6}$$

$$\varepsilon_t = \rho\varepsilon_{t-1} + \mu_t;\ \mu_t \sim N(0, \sigma^2) \tag{7}$$

where β_0 and β_1 are parametric coefficients, $s(\text{Temperature}_t)$, $s(\text{Flow}_t)$, and $s(\text{Tide}_t)$ indicate smooth non-

parametric functions for daily mean water temperature, river flow, and tidal amplitude fitted using thin plate regression splines. $Year_t$ indicates a categorical non-smooth term for year (2019 and 2020). Temporal autocorrelation of the residuals ε_t was modeled using the first-order autoregressive structure, AR(1), where ρ is the autoregressive coefficient. The best model was selected by comparing AICc. After the assumptions of homoskedasticity, uncorrelatedness, and normality of residuals were verified, the significance of the model coefficients was assessed. Despite having a similar collection date, 1 fish dispersed substantially later than the overall median dispersal date (z-score = 3.53). This individual was regarded as an outlier and removed from the analysis, as it would have substantially skewed the relationship between dispersal timing and environmental drivers.

The compensatory growth hypothesis was tested using 2-way ANOVA with a gamma distribution and a log link function to detect differences in larval and juvenile growth rates of age-0 juveniles across migration contingents, years (2019 and 2020), and their interaction (step G in Fig. 2). A post hoc Tukey test was employed for multiple comparisons of these variables across contingents within each year using the 'emmeans' R package (Lenth et al. 2022).

3. RESULTS

3.1. Migration contingents

Time-series clustering of otolith Sr and Ba transects with DTW detected 3 and 4 distinct clusters, or migration contingents, in 2019 and 2020, respectively (Fig. 3; equivalent plot in element:Ca ratios shown in Fig. S7). However, the first cluster in 2019 exhibited 2 separate migration contingents with large differences in Sr and Ba concentrations, leading to a total of 4 dominant migration contingents for both 2019 and 2020. The first group showed low Sr concentration, indicative of lifetime freshwater habitat use, and was assigned 'freshwater residents'. The second group, referred to as 'oligohaline migrants', showed an abrupt shift in Sr concentration that leveled off at around 1500 ppm, indicating dispersal to oligohaline habitats (mean dispersal size: 42.5 mm [2019]; 14.3 mm [2020]). The third group, assigned 'large mesohaline migrants', initially showed low Sr concentrations, and then a marked increase later in life and consistently high Sr concentration around 2500 ppm, indicating dispersal and subsequent mesohaline habitat use (mean dispersal size: 51.2 mm [2019]; 46.0 mm [2020]). The fourth and final group, assigned 'small mesohaline migrants', displayed Sr concentrations that increased rapidly early in life and were persistently high, reflecting dispersal to mesohaline habitats at a small size (mean dispersal size: 21.3 mm [2019]; 20.5 mm [2020]). A small number of samples (n = 18 of 131 total) displayed consistently low Sr concentrations despite being collected in brackish-water habitats. These fish were considered recent migrants whose otolith chemical signature did not yet reflect the ambient condition of the brackish-water collection site. Thus, to prevent erroneous contingent assignment, these samples were excluded from cluster analysis and were manually assigned a contingent membership based on their collection site and total length (n = 11 to 'oligohaline migrants' and n = 7 to 'large mesohaline migrants').

3.2. Effect of larval growth and early life history characteristics on migration contingents

Multinomial logistic regression analysis indicated that covarying larval environmental conditions were associated with contingent membership in 2020 but not in 2019, where only larval growth explained contingent membership (Table 1). In 2019, fish that showed the slowest larval growth rates were more likely to become oligohaline migrants, although the relationship with larval growth was less apparent with other migration contingents (Fig. 4A). For 2020 samples, larval growth, and a principal component defined by larval environmental characteristics (strong loadings of hatch dates and experienced temperature inversely covarying with flow and chl *a*; see Fig. S4) were retained as important variables (Table 1). Predicted contingent membership probabilities indicated that oligohaline migrants arose from individuals with the slowest larval growth and later hatch dates associated with high temperature, low flow, and low chl *a* concentration (Fig. 4B). In contrast, individuals that exhibited the highest larval growth and early hatch dates during a period of low temperature, high flow, and high chl *a* concentration migrated to mesohaline habitats at a large size (Fig. 4B). Freshwater residents and small mesohaline migrants arose from individuals exhibiting intermediate larval growth and hatch dates.

3.3. Dispersal timing and environmental drivers

The changepoint analysis combined with RF habitat assignment (overall classification accuracy: 0.97;

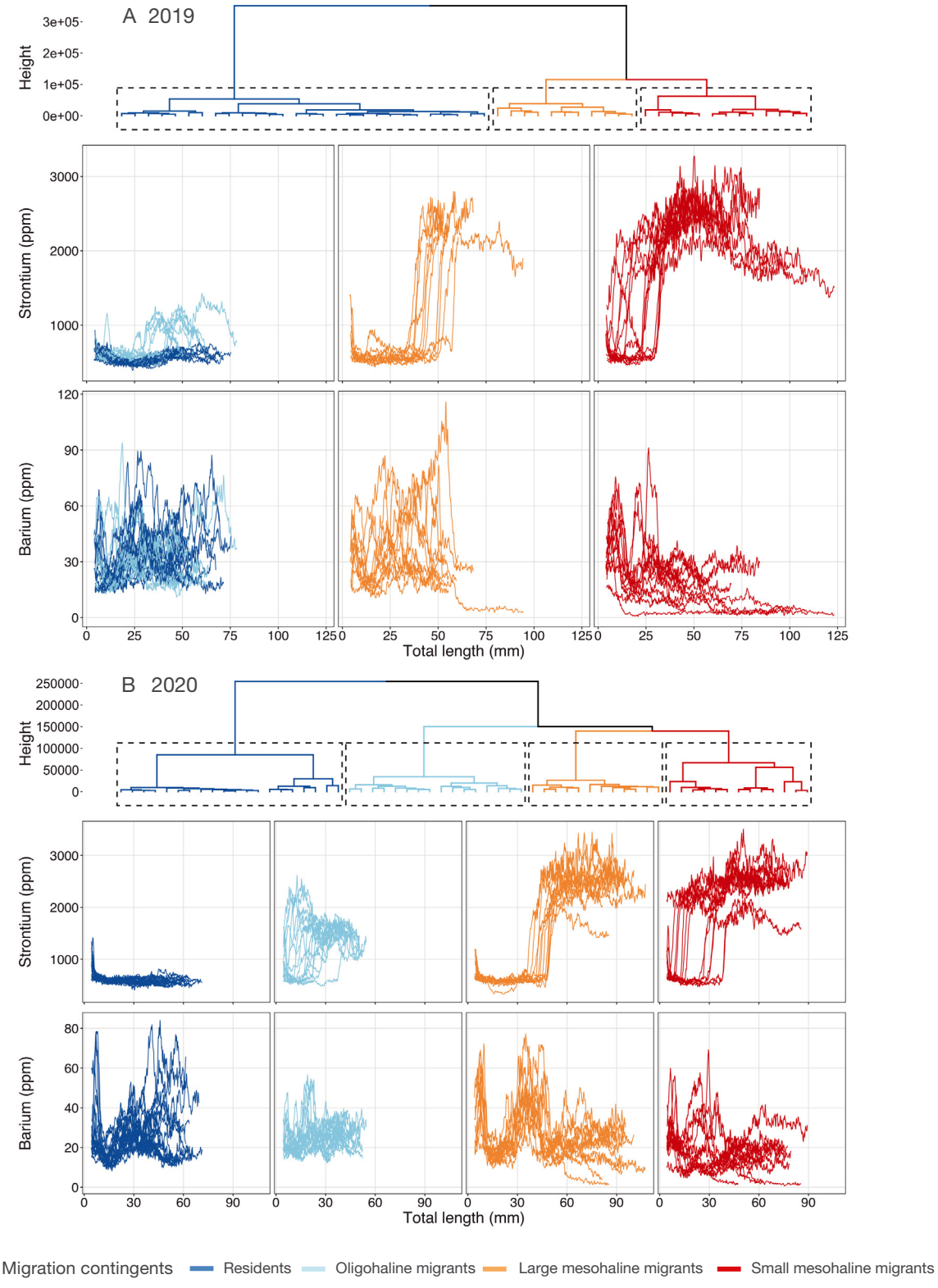

Fig. 3. Hierarchical dynamic time warping clustering results using otolith Sr and Ba transects of Hudson River juvenile striped bass for (A) 2019 and (B) 2020. Different colors and dashed rectangles on the dendrogram illustrate distinct clusters (i.e. migration contingents): residents (dark blue), oligohaline migrants (light blue), large mesohaline migrants (yellow), and small mesohaline migrants (red)

Table S2) detected the size and age (date) at dispersal to brackish-water habitats. Dispersal events in 2019 were spaced out in time from late June to late August 2019, with no more than 27% of total fish emigrating from freshwater in any given week (Fig. 5A). While there were a few major peaks in both flow and tidal amplitude, there was no clear relationship between these environmental drivers and the timing of dispersal. In 2020, the majority of fish (>70%) emigrated from freshwater habitats within a 2 wk window from 29 June to 13 July 2020, coinciding with a period of high flow and high tidal amplitude (Fig. 5B). The final GAMM of the effect of environmental conditions on dispersal timing included daily tidal amplitude, although the coefficient estimate of the smooth term was not statistically significant (effective degrees of freedom = 1, F = 0.54, p = 0.467; Table S3).

Table 1. Akaike's information criterion corrected for small sample size (AICc) rankings of the multinomial logistic regression model to assess the probability of migration contingent membership in relation to larval growth, hatch dates, and early life environmental conditions of striped bass. The first principal component (PC1) includes hatch dates and environmental conditions experienced during the first 30 d of life (i.e. mean water temperature, flow, and chlorophyll *a*). ΔAICc shows the differences in AICc between the best model (rank 1) and a given model

Year	Rank	Model	df	AICc	ΔAICc
2019	1	Larval growth	6	191.33	0.00
	2	Larval growth + PC1	9	195.40	4.07
	3	Intercept	3	195.94	4.61
	4	PC1	6	199.89	8.57
2020	1	Larval growth + PC1	9	136.65	0.00
	2	PC1	6	154.46	17.81
	3	Larval growth	6	163.42	26.77
	4	Intercept	3	176.25	39.60

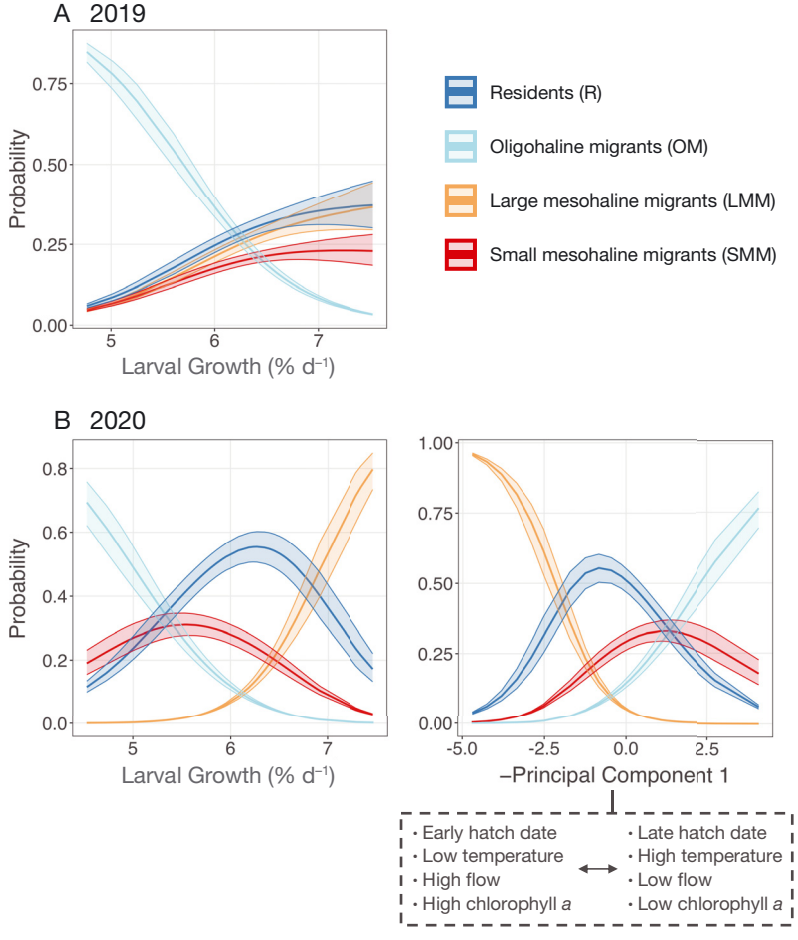

Fig. 4. Predicted migration contingent probabilities as a function of specific larval growth and early life characteristics (principal component 1, PC1) of juvenile striped bass in (A) 2019 and (B) 2020 from multinomial logistic regression analysis. PC1 included hatch dates and environmental conditions (water temperature, flow, and chlorophyll *a*) experienced by individuals during the first 30 d of life. Shadings indicate 95% confidence intervals. Note that the direction of the *x*-axis for the PC1 score was reversed to facilitate interpretation: higher PC scores reflect individuals with later hatch dates exposed to high temperature, low flow, and low chlorophyll *a* concentration. Because larval growth was the only predictor retained as an important variable explaining contingent membership in 2019 (see Table 1), the relationship between contingent membership probability and PC1 is not displayed for 2019

3.4. WLIS entry

With the exception of 1 fish that entered the WLIS during the late-larval phase (TL < 15 mm), the majority of the fish (93% of total samples) that were captured within the WLIS entered during their juvenile phase (TL > 30 mm; Fig. 6A). The estimated coefficient of the GLM showed a significant negative relationship between the initial dispersal size to brackish habitats and the number of days spent in brackish water before entering WLIS (coefficient ± SE = −0.03 ± 0.01, p = 0.004; Fig. 6B).

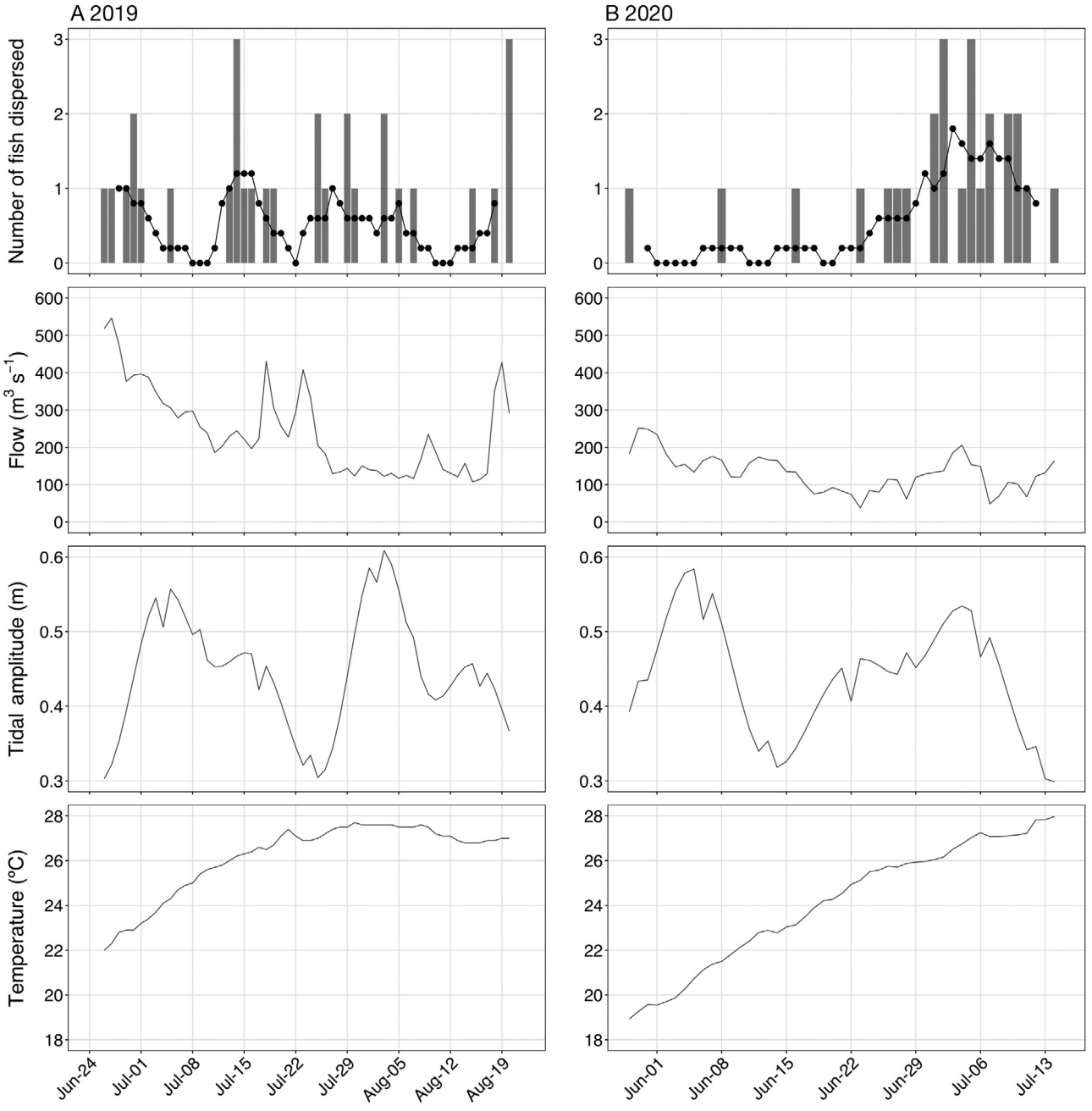

Fig. 5. Daily number of striped bass dispersed to mesohaline habitats displayed with daily mean flow, tidal amplitude, and water temperature for (A) 2019 and (B) 2020. Solid circles and lines illustrate the smoothed 5 d centered moving average of the daily number of fish dispersed to mesohaline habitats. Note that the scales of the *x*-axes differ between years

3.5. Compensatory growth

Significant differences in larval growth rates were detected between contingents (2-way ANOVA, $F_{3,123} = 10.70$, $p < 0.001$) and years ($F_{1,123} = 16.83$, $p < 0.001$), but not their interaction ($F_{3,123} = 1.92$, $p = 0.130$; Fig. 7A). In both years, oligohaline migrants exhibited significantly slower growth rates compared to residents (Tukey test, $p_{2019} = 0.048$, $p_{2020} = 0.008$) and large mesohaline migrants ($p_{2019} = 0.044$, $p_{2020} < 0.001$). Larval growth rates were on average higher in 2019 compared to 2020 ($p < 0.001$). For juvenile growth rates, no significant contingent (2-way ANOVA, $F_{3,107} = 1.28$, $p = 0.286$), year ($F_{1,107} = 0.91$, $p = 0.341$), or interaction effects ($F_{3,107} = 1.81$, $p = 0.150$) were detected (Fig. 7B).

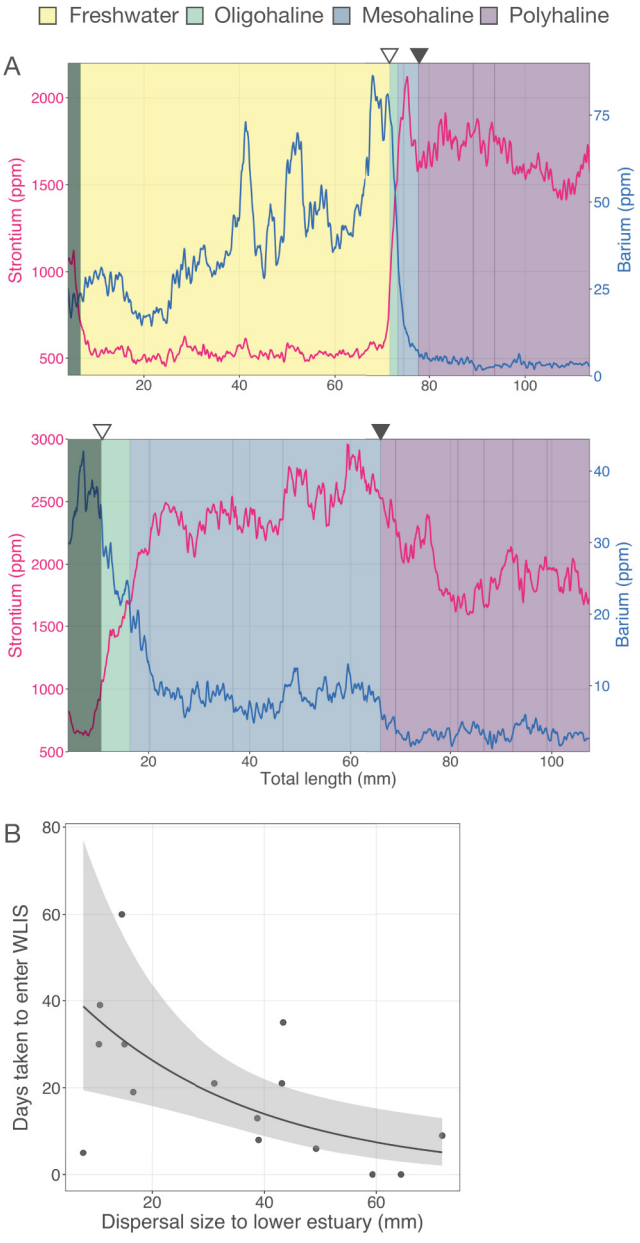

Fig. 6. (A) Example otolith Sr (pink) and Ba (blue) transects and predicted habitats of 2 juvenile striped bass that dispersed to brackish habitats during the juvenile (top) and larval (bottom) phases. Background colors illustrate predicted habitats from changepoint analysis and random forest classification. Open and solid triangles between the 2 habitats indicate the dispersal size to brackish habitats and polyhaline habitats (i.e. western Long Island Sound, WLIS), respectively. Note that otolith chemistry in the shaded region near the early life stage may be maternally derived and was not considered as a changepoint. (B) Relationship between the dispersal size to brackish habitats and the total number of days spent in the lower Hudson River Estuary before entering the WLIS for striped bass collected in the WLIS in 2019 and 2020. The solid line and shaded area indicate the predicted value and 95% confidence intervals from the generalized linear model with a negative binomial distribution

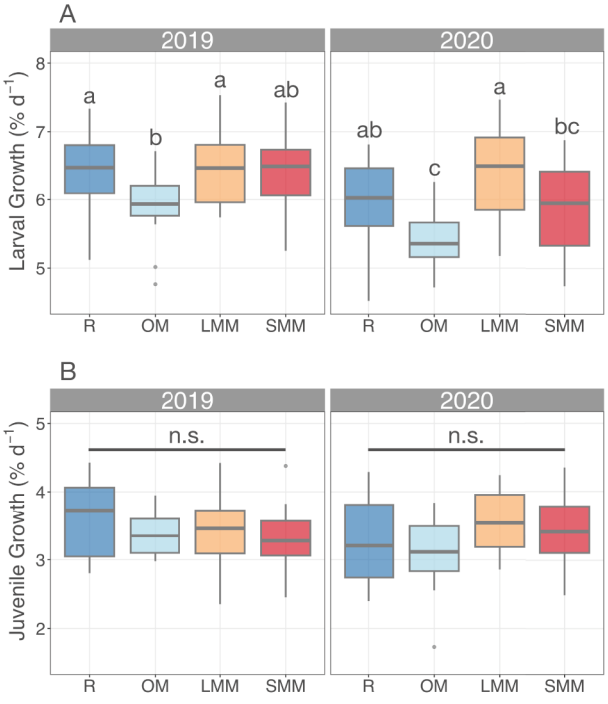

Fig. 7. Specific (A) larval and (B) juvenile growth rates of resident (R), oligohaline migrant (OM), large mesohaline migrant (LMM), and small mesohaline migrant (SMM) striped bass in 2019 and 2020. Different letters above each box show significant growth differences based on post hoc Tukey tests ($p < 0.05$). NS = no significant differences detected. The bottom of the box indicates the first quartile (*Q*1), the horizontal line the second quartile (Q2 = median), and the top the third quartile (Q3). The interquartile range (IQR) is calculated as Q3 − Q1, and the whiskers are defined as Q1 − 1.5×IQR for the lower whisker and Q3 + 1.5×IQR for the upper whisker. Solid circles correspond to observations less than Q1 − 1.5×IQR or greater than Q3 + 1.5×IQR

4. DISCUSSION

Partial migration of juvenile HR striped bass was conditionally influenced by larval growth and facultatively controlled by environmental drivers. We uncovered 4 dominant early migration contingents for 2 successive years with contrasting hydrologic conditions and juvenile densities. In both years, migration contingents were similarly associated with larval growth: oligohaline migrants arose from individuals with the slowest larval growth, whereas those with the fastest larval growth migrated to mesohaline habitats at a larger size after a prolonged period of freshwater residency. Intermediate larval growth rates were associated with lifetime freshwater residency in the dry 2020 season, but not in the wet 2019 season. Differences in the timing of hatch in the dry year may have indirectly affected migration contin-

gents by exposing larvae to various environmental conditions. Dispersal timing coincided with a period of relatively high freshwater and tidal flow in the dry 2020 season, although no clear relationship was found between dispersal timing and environmental variables for the wet 2019 season. In both years, we found no evidence of compensatory growth in slow-growing oligohaline migrants following dispersal to brackish environments.

4.1. Early migration contingents in juvenile striped bass

High-resolution otolith microchemistry data coupled with DTW cluster analysis uncovered distinct early migration contingents in juvenile striped bass in the HR (Fig. 3). These contingents were discrete in their dispersal sizes and habitat destinations. Similar early migration contingents have been reported for juvenile striped bass populations in the Chesapeake Bay (Conroy et al. 2015), St. Lawrence Estuary (Morissette et al. 2016, Vanalderweireldt et al. 2019), and Albemarle Sound (Mohan et al. 2015), with some juveniles remaining in their natal freshwater or oligohaline habitats while others migrate downstream into higher-salinity habitats. This suggests that partial migration during the early life stages could be prevalent among striped bass populations along the Atlantic coast, which may have developed as a plastic response to nonstationary environments (Kerr et al. 2010).

Dispersal timing and behaviors were informed by otolith Sr and Ba, which have been used extensively to reconstruct fish movement across salinity gradients (Elsdon et al. 2008, Walther & Limburg 2012, Walther 2019). Sr generally shows a positive relationship with salinity, whereas Ba often behaves in an inverse manner to Sr, with higher concentrations in low to mid-salinity and minimal concentrations in marine waters (Walther & Limburg 2012, Nelson & Powers 2020). A similar relationship between Sr and Ba and salinity was observed in the otoliths of juvenile striped bass in the HR (Fig. 3; Fig. S6B). The rapid increase in otolith Ba just before the increase in otolith Sr could be reflecting the mid-salinity peak of Ba in the HR (Figs. 3 & 6A). This is because when riverine suspended particulate matter (SPM) initially meets the salt wedge, ion exchange between seawater and SPM induces desorption and release of free Ba, leading to a peak Ba in these moderate salinities (Coffey et al. 1997, Walther & Limburg 2012, Nelson & Powers 2020). This unique feature allowed Ba to be a useful tracer in reconstructing juvenile movement between mesohaline and polyhaline habitats where Sr was less informative (Fig. 6A; Fig. S6).

The dispersal sizes of small and large mesohaline migrants were similar in both years (Fig. 3). However, the dispersal size of oligohaline migrants was substantially larger in 2019 than in 2020, which could be an artifact of our approach that relied on otolith chemistry to infer movement across salinity gradients. Given the higher flow in 2019, the salinity gradient in the estuary may have been too small to detect any spatial differences between freshwater and downstream habitats, biasing the dispersal size higher (later in the season). The lower otolith Sr concentration of oligohaline migrants in 2019 compared to 2020, as well as the initial grouping of these fish with freshwater residents could also be explained by the high flow in 2019 (Fig. 3). Further, because oligohaline migrants in 2019 were collected in the transition zone under high flow conditions (Fig. 1), the decrease in otolith Sr immediately before capture likely reflected changes in ambient salinity rather than upstream migration into freshwater habitats. Still, identified migration contingents were broadly consistent between years despite contrasting hydrological conditions and age-0 juvenile recruitment levels (Fig. S1).

How striped bass recruit to WLIS nurseries via the East River has been a long-standing question (Dovel 1992, Dunning et al. 2009). Here, size at ingress to WLIS was broad, but mostly occurred during the juvenile phase (TL > 30 mm, Fig. 6A). However, we cannot rule out the possibility that variation in recruitment size to the WLIS nursery could be explained by juveniles entering the WLIS from other systems, namely the nearby Connecticut River, where adult striped bass are also present (Davis et al. 2012). Nonetheless, elemental concentrations measured near the otolith core region indicated no evidence of an alternative spawning source (Fig. S3). Furthermore, no direct evidence of striped bass spawning in the Connecticut River has been found (Waldman et al. 1988, Gephard & McMenemy 2004), and the majority of WLIS-recruited fish are thought to have originated in the HR.

For individuals that recruited to the WLIS, the initial dispersal size to brackish habitats appeared to influence the amount of time spent in the lower HR before entering WLIS, with smaller dispersers spending more time in the lower HR, and vice versa for larger dispersers (Fig. 6B). A plausible explanation for this relationship could be that the greater swimming ability of larger fish facilitated a shorter transit time

through the East River, where the net tides flow against transit, back towards the lower HR estuary (Blumberg & Pritchard 1997, Blumberg et al. 1999). Smaller fish, on the other hand, may need to adjust their vertical position in the water column to utilize the eastward residual flow in the upper water column and passively transition through this high-velocity strait, delaying WLIS entry.

4.2. Partial migration as a conditional strategy

Early migration contingents of HR striped bass were associated with early growth rates (Fig. 4), corroborating past studies across varied taxa (Jonsson & Jonsson 1993, Chapman et al. 2012, Dodson et al. 2013, Secor 2015) and supporting a growth-mediated migration threshold for juvenile striped bass. The propensity to migrate early or to migrate to proximate oligohaline habitats was related to slower larval growth, whereas freshwater residency or delayed migration to distant mesohaline habitats was associated with faster larval growth (Fig. 4). Fast-growers thus forgo migration, whereas slow-growers undertake a riskier strategy to search for suitable habitats to enhance future fitness outcomes. A similar relationship between early growth and migration propensity has been observed in several freshwater and coastal species including the congeneric white perch (Kraus & Secor 2004, Kerr & Secor 2010) and striped bass from the Chesapeake Bay (Conroy et al. 2015) and St. Lawrence Estuary populations (Vanalderweireldt et al. 2019).

Somatic growth rates may have a direct effect on otolith chemistry (Miller & Hurst 2020, Hüssy et al. 2021). Specifically, Sr and Ba exhibit decreasing partitioning from water to otolith with higher growth rates (Sadovy & Severin 1992, Walther et al. 2010, Miller & Hurst 2020), whereas Mg incorporation is positively associated with faster growth (Sturrock et al. 2015, Limburg et al. 2018). Still, the difference in water chemistry across habitats is likely greater than the variability related to growth (Elsdon & Gillanders 2003, Reis-Santos et al. 2013), and it is unlikely that the observed larval growth differences led to biased contingent assignments. Furthermore, most variation in otolith Sr occurred during the juvenile phase, when growth rates were similar across contingents (Fig. 7B).

Protracted spawning of striped bass exposes larval cohorts to various environmental and foraging conditions, leading to extreme variation in larval growth rates (Houde 1997, Secor 2000). While we detected no significant effects of hatch dates and early life experiences on early growth (see Text S3), early growth and hatch dates were closely related in 2020, with the fast-growing large mesohaline migrants hatching significantly earlier than the slow-growing oligohaline migrants (Fig. 4B; Fig. S5A). Despite being exposed to a significantly lower temperature and higher flow, the fast-growing early-hatched cohort experienced higher chl *a* concentrations compared to their later-hatched slow-growing peers, which, if associated with secondary production, may have resulted in their accelerated larval growth rates (Fig. 4B; Fig. S5). Intraspecific competition may also have played an important role where early-hatched cohorts preoccupied favorable habitats for early growth, forcing later-hatched cohorts to utilize suboptimal habitats (MacCall 1990, Chapman et al. 2012, Mohan et al. 2015). This density-dependent effect could be important, especially considering the strong recruitment in 2020 (Fig. S1A). We detected significant effects of early life experiences on larval growth (see Text S3), although hatch dates and early life experiences were not selected as a significant predictor for contingent membership in 2019 (Fig. 4, Table 1). These results could imply that environmental conditions influenced larval growth, which in turn affected juvenile migration propensity.

Environmental drivers did not appear to have a significant effect on dispersal timing in either year (Fig. 5), although inferences are limited to the samples analyzed and do not necessarily apply to the whole population. Circumstantially, a major dispersal event coincided with a period of relatively high freshwater and tidal flow in 2020, consistent with a larval dispersal event described for striped bass in the Chesapeake Bay (Conroy et al. 2015; Fig. 5). One plausible explanation for this relationship could be that the growth-mediated migration threshold interacts with environmental drivers, wherein the threshold value is influenced by river and tidal flow (Pulido 2011). Thus, high flow and tidal currents could shift the growth threshold, acting as a trigger that initiates the dispersal behavior of individuals below a specific growth threshold (Nathan et al. 2008, Conroy et al. 2015). Alternatively, the apparent relationship between dispersal and flow events could simply be due to displacement of larvae downstream.

4.3. Consequences of migration

We predicted accelerated growth to occur in more productive brackish habitats as an immediate consequence of migration. Specifically, we hypothesized

that oligohaline migrants would compensate for their slower larval growth by exhibiting higher post-dispersal juvenile growth compared to other migration contingents. As determined by larval growth comparison, oligohaline migrants were significantly slower in growth compared to their peers prior to dispersal (Fig. 7A). While the slow-growing oligohaline migrants demonstrated similar juvenile growth to their counterparts in both years following dispersal to brackish habitats, we found no evidence of post-dispersal accelerated growth (i.e. compensatory growth; Metcalfe & Monaghan 2001; Fig. 7B). Such compensatory responses have been reported in a range of fishes, including congeneric white perch in Chesapeake Bay (Kerr & Secor 2009) and HR (Gallagher et al. 2018). We predicted similar compensatory responses for HR striped bass juveniles given that oligohaline and mesohaline habitats are generally more productive than freshwater habitats, which may provide greater foraging opportunities for dispersers (Sirois & Fredrick 1978, Howarth et al. 2006). The benefit of accelerated growth following migration to brackish habitats could be outweighed by the energetic cost of migration and osmoregulatory responses to higher salinity (Chapman et al. 2012). It is also important to note that our approach considers only the survivors, and the potential cost associated with migration requires further investigation, especially given the increased abundance of piscivorous predators (e.g. bluefish *Pomatomus saltatrix*) with greater salinity and depth (Juanes et al. 1993, Buckel et al. 1999).

Research on a congeneric species, white perch, could inform how partial migration early in life could have important consequences on the HR adult striped bass population dynamics. Adult white perch growth and maturation rates vary according to early migration contingents (Kraus & Secor 2004, Kerr et al. 2010, Gallagher et al. 2018). In this study, HR striped bass early-life partial migration led to a wide range of nursery habitat use patterns, including freshwater, brackish, and coastal habitats (Fig. 3). Such spatial 'bet-hedging', stemming from diverse early migration contingents, leads to portfolio effects that stabilize populations in highly varied estuarine environments (Schindler et al. 2010, Secor 2015, Stier et al. 2020). For conservation and management applications, future efforts should focus on assessing how these diverse nurseries differentially produce individuals that recruit to the adult striped bass population (Beck et al. 2001, Kraus & Secor 2005).

Importantly, long-term increases in freshwater flow and temperature in the HR due to climate change may modify striped bass partial migration responses and population dynamics (Najjar et al. 2009, Seekell & Pace 2011; Fig. S1). Earlier spawning of adult striped bass is predicted with increased temperature (Pan et al. 2023). Shifts in the timing of spawning and hatching will expose larvae to different environmental conditions, affecting larval growth and consequently juvenile partial migration dynamics. Climate change is predicted to increase freshwater flow, which may increase the proportion of the migratory contingent through the influence on the growth-mediated migration threshold and/or by displacing larvae downstream (Pulido 2011, Conroy et al. 2015). Furthermore, because flow is strongly and inversely related to primary productivity in the HR (Howarth et al. 2000, Gallagher & Secor 2018), projected higher flow could result in slower larval growth, favoring the migratory contingent. Given the unique and complementary roles that diverse early migration traits play in the population dynamics (Kraus & Secor 2004, Kerr et al. 2010), a potential decline in the freshwater resident contingent could jeopardize the long-term persistence of the HR striped bass population. Thus, understanding and preserving key drivers that promote diverse life history traits could provide valuable insights for sustainable fisheries and conservation strategies for this important species in the face of climate change.

Acknowledgements. We thank Michelle Sluis for training and assistance with the LA-ICP-MS analysis. This manuscript benefited greatly from insights and inputs from Reginal Harrell, Lisa Kerr, David Nelson, Michael Wilberg, and Ryan Woodland. We also thank the Editor and reviewers for their helpful comments that significantly improved this paper. This research was funded by the Hudson River Foundation under grant number 004/19A. K.A. was financially supported by a fellowship from the Japan Student Services Organization.

LITERATURE CITED

Aghabozorgi S, Seyed Shirkhorshidi A, Ying Wah T (2015) Time-series clustering — a decade review. Inf Syst 53: 16–38

Aubin-Horth N, Dodson JJ (2004) Influence of individual body size and variable thresholds on the incidence of a sneaker male reproductive tactic in Atlantic salmon. Evolution 58:136–144

Beck MW, Heck KL, Able KW, Childers DL and others (2001) The identification, conservation, and management of estuarine and marine nurseries for fish and invertebrates. BioScience 51:633–641

Berg JE, Hebblewhite M, St. Clair CC, Merrill EH (2019) Prevalence and mechanisms of partial migration in ungulates. Front Ecol Evol 7:325

Blumberg AF, Pritchard DW (1997) Estimates of the transport through the East River, New York. J Geophys Res 102:5685–5703

Blumberg AF, Khan LA, St. John JP (1999) Three-dimensional hydrodynamic model of New York Harbor region. J Hydraul Eng 125:799–816

Boreman J, Klauda RJ (1988) Distributions of early life stages of striped bass in the Hudson River Estuary, 1974–1979. Am Fish Soc Monogr 4:53–58

Breiman L (2001) Random forests. Mach Learn 45:5–32

Buckel JA, Conover DO, Steinberg ND, McKown KA (1999) Impact of age-0 bluefish (*Pomatomus saltatrix*) predation on age-0 fishes in the Hudson River estuary: evidence for density-dependent loss of juvenile striped bass (*Morone saxatilis*). Can J Fish Aquat Sci 56:275–287

Campana SE (1990) How reliable are growth back-calculations based on otoliths? Can J Fish Aquat Sci 47: 2219–2227

Chapman BB, Brönmark C, Nilsson JÅ, Hansson LA (2011) The ecology and evolution of partial migration. Oikos 120:1764–1775

Chapman BB, Hulthén K, Brodersen J, Nilsson PA, Skov C, Hansson LA, Brönmark C (2012) Partial migration in fishes: causes and consequences. J Fish Biol 81:456–478

Coffey M, Dehairs F, Collette O, Luther G, Church T, Jickells T (1997) The behaviour of dissolved barium in estuaries. Estuar Coast Shelf Sci 45:113–121

Conroy CW, Piccoli PM, Secor DH (2015) Carryover effects of early growth and river flow on partial migration in striped bass *Morone saxatilis.* Mar Ecol Prog Ser 541: 179–194

Davis JP, Schultz ET, Vokoun JC (2012) Striped bass consumption of blueback herring during vernal riverine migrations: Does relaxing harvest restrictions on a predator help conserve a prey species of concern? Mar Coast Fish 4:239–251

Dodson JJ, Aubin-Horth N, Thériault V, Páez DJ (2013) The evolutionary ecology of alternative migratory tactics in salmonid fishes: alternative migratory tactics as threshold traits. Biol Rev Camb Philos Soc 88:602–625

Dovel WL (1992) Movement of immature striped bass in the Hudson River Estuary. In: Smith CL (ed) Estuarine research in the 1980s. Hudson River Environmental Society, Seventh Symposium on Hudson River Ecology. State University of New York Press, Albany, NY, p 276–302

Dunning DJ, Ross QE, McKown KA, Socrates JB (2009) Effect of striped bass larvae transported from the Hudson River on juvenile abundance in western Long Island Sound. Mar Coast Fish 1:343–353

Elsdon TS, Gillanders BM (2003) Relationship between water and otolith elemental concentrations in juvenile black bream *Acanthopagrus butcheri.* Mar Ecol Prog Ser 260: 263–272

Elsdon TS, Gillanders BM (2005) Strontium incorporation into calcified structures: separating the effects of ambient water concentration and exposure time. Mar Ecol Prog Ser 285:233–243

Elsdon TS, Wells BK, Campana SE, Gillanders BM and others (2008) Otolith chemistry to describe movements and life-history parameters of fishes: hypotheses, assumptions, limitations and inferences. Oceanogr Mar Biol Annu Rev 46:297–330

Forseth T, Naesje TF, Jonsson B, Hårsaker K (1999) Juvenile migration in brown trout: a consequence of energetic state. J Anim Ecol 68:783–793

Gahagan BI, Fox DA, Secor DH (2015) Partial migration of striped bass: revisiting the contingent hypothesis. Mar Ecol Prog Ser 525:185–197

Gallagher BK, Secor DH (2018) Intensified environmental and density-dependent regulation of white perch recruitment after an ecosystem shift in the Hudson River Estuary. Can J Fish Aquat Sci 75:36–46

Gallagher BK, Piccoli PM, Secor DH (2018) Ecological carryover effects associated with partial migration in white perch (*Morone americana*) within the Hudson River Estuary. Estuar Coast Shelf Sci 200:277–288

Gephard S, McMenemy J (2004) An overview of the program to restore Atlantic salmon and other diadromous fishes to the Connecticut River with notes on the current status of these species in the river. Am Fish Soc Monogr 9: 287–317

Hastie T, Tibshirani R, Friedman J (2009) The elements of statistical learning: data mining, inference, and prediction. Springer Science & Business Media, New York, NY

Hegg JC, Kennedy BP (2021) Let's do the time warp again: non-linear time series matching as a tool for sequentially structured data in ecology. Ecosphere 12:e03742

Hegg JC, Kennedy BP, Chittaro P (2019) What did you say about my mother? The complexities of maternally derived chemical signatures in otoliths. Can J Fish Aquat Sci 76:81–94

Houde ED (1997) Patterns and consequences of selective processes in teleost early life histories. In: Chambers RC, Trippel EA (eds) Early life history and recruitment in fish populations. Fish and Fisheries Series. Chapman & Hall, Dordrecht, p 173–196

Houde ED, Morin L (1990) Temperature effects on otolith daily increment deposition in striped bass and white perch larvae. In: Proc Meeting of the International Council for the Exploration of the Sea. ICES, Copenhagen

Howarth RW, Swaney DP, Butler TJ, Marino R (2000) Climatic control on eutrophication of the Hudson River Estuary. Ecosystems 3:210–215

Howarth RW, Marino R, Swaney DP, Boyer EW (2006) Wastewater and watershed influences on primary productivity and oxygen dynamics in the lower Hudson River Estuary. In: Levinton JS, Waldman JR (eds) The Hudson River estuary. Cambridge University Press, Cambridge, p 121–139

Hüssy K, Limburg KE, de Pontual H, Thomas ORB and others (2021) Trace element patterns in otoliths: the role of biomineralization. Rev Fish Sci Aquac 29:445–477

Jonsson B, Jonsson N (1993) Partial migration: niche shift versus sexual maturation in fishes. Rev Fish Biol Fish 3: 348–365

Juanes F, Marks RE, McKown KA, Conover DO (1993) Predation by age-0 bluefish on age-0 anadromous fishes in the Hudson River Estuary. Trans Am Fish Soc 122: 348–356

Kalish JM (1990) Use of otolith microchemistry to distinguish the progeny of sympatric anadromous and non-anadromous salmonids. Fish Bull 88:657–666

Kerr LA, Secor DH (2009) Bioenergetic trajectories underlying partial migration in Patuxent River (Chesapeake Bay) white perch (*Morone americana*). Can J Fish Aquat Sci 66:602–612

Kerr LA, Secor DH (2010) Latent effects of early life history on partial migration for an estuarine-dependent fish. Environ Biol Fishes 89:479–492

Kerr LA, Secor DH, Piccoli PM (2009) Partial migration of fishes as exemplified by the estuarine-dependent white perch. Fisheries 34:114–123

Kerr LA, Cadrin SX, Secor DH (2010) The role of spatial dynamics in the stability, resilience, and productivity of an estuarine fish population. Ecol Appl 20:497–507

Killick R, Eckley IA (2014) Changepoint: an R package for changepoint analysis. J Stat Soft 58(3):1–19

Kraus RT, Secor DH (2004) Dynamics of white perch *Morone americana* population contingents in the Patuxent River estuary, Maryland, USA. Mar Ecol Prog Ser 279:247–259

Kraus RT, Secor DH (2005) Application of the nursery-role hypothesis to an estuarine fish. Mar Ecol Prog Ser 291: 301–305

Lenth R, Singmann H, Love J, Buerkner P, Herve M (2022) Emmeans: estimated marginal means, aka least-squares means. R package v.1.7.5. https://CRAN.R-project.org/package=emmeans

Limburg KE, Wuenschel MJ, Hüssy K, Heimbrand Y, Samson M (2018) Making the otolith magnesium chemical calendar-clock tick: plausible mechanism and empirical evidence. Rev Fish Sci Aquacult 26:479–493

Lüdecke D (2018) Ggeffects: tidy data frames of marginal effects from regression models. J Open Source Softw 3: 772

Lundberg P (1988) The evolution of partial migration in birds. Trends Ecol Evol 3:172–175

MacCall AD (1990) Dynamic geography of marine fish populations. University of Washington Press, Seattle, WA

Mansueti R (1958) Eggs, larvae and young of the striped bass, *Roccus saxatilis*. Contribution no 112. Chesapeake Biological Laboratory, Maryland Department of Research and Education, Solomons, MD

Menz MHM, Reynolds DR, Gao B, Hu G, Chapman JW, Wotton KR (2019) Mechanisms and consequences of partial migration in insects. Front Ecol Evol 7:403

Metcalfe NB, Monaghan P (2001) Compensation for a bad start: grow now, pay later? Trends Ecol Evol 16:254–260

Metcalfe NB, Huntingford FA, Graham WD, Thorpe JE (1989) Early social status and the development of life-history strategies in Atlantic salmon. Proc R Soc B 236:7–19

Miller JA, Hurst TP (2020) Growth rate, ration, and temperature effects on otolith elemental incorporation. Front Mar Sci 7:320

Mohan JA, Halden NM, Rulifson RA (2015) Habitat use of juvenile striped bass *Morone saxatilis* (Actinopterygii: Moronidae) in rivers spanning a salinity gradient across a shallow wind-driven estuary. Environ Biol Fishes 98: 1105–1116

Morissette O, Lecomte F, Verreault G, Legault M, Sirois P (2016) Fully equipped to succeed: migratory contingents seen as an intrinsic potential for striped bass to exploit a heterogeneous environment early in life. Estuar Coasts 39:571–582

Morissette O, Lecomte F, Vachon N, Drouin A, Sirois P (2021) Quantifying migratory capacity and dispersal of the invasive tench (*Tinca tinca*) in the St. Lawrence River using otolith chemistry. Can J Fish Aquat Sci 78: 1628–1638

Najjar R, Patterson L, Graham S (2009) Climate simulations of major estuarine watersheds in the Mid-Atlantic region of the US. Clim Change 95:139–168

Nathan R, Getz WM, Revilla E, Holyoak M, Kadmon R, Saltz D, Smouse PE (2008) A movement ecology paradigm for unifying organismal movement research. Proc Natl Acad Sci USA 105:19052–19059

NEFSC (2019) 66th Northeast regional stock assessment workshop (66th SAW) assessment report. Ref Doc 19-08. US Department of Commerce, Northeast Fisheries Science Center, Woods Hole, MA

Nelson TR, Powers SP (2020) Elemental concentrations of water and otoliths as salinity proxies in a Northern Gulf of Mexico estuary. Estuar Coasts 43:843–864

Nordeng H (1983) Solution to the 'char problem' based on Arctic char (*Salvelinus alpinus*) in Norway. Can J Fish Aquat Sci 40:1372–1387

O'Connor CM, Norris DR, Crossin GT, Cooke SJ (2014) Biological carryover effects: linking common concepts and mechanisms in ecology and evolution. Ecosphere 5:28

Olsson IC, Greenberg LA, Bergman E, Wysujack K (2006) Environmentally induced migration: the importance of food. Ecol Lett 9:645–651

Pace ML, Findlay SEG, Fischer D (1998) Effects of an invasive bivalve on the zooplankton community of the Hudson River. Freshw Biol 39:103–116

Pan X, Arsenault S, Rokosz K, Chen Y (2023) Spatial variability of striped bass spawning responses to climate change. Glob Ecol Conserv 42:e02405

Paton C, Hellstrom J, Paul B, Woodhead J, Hergt J (2011) Iolite: freeware for the visualisation and processing of mass spectrometric data. J Anal At Spectrom 26:2508

Pechenik JA (2006) Larval experience and latent effects — metamorphosis is not a new beginning. Integr Comp Biol 46:323–333

Peller T, Guichard F, Altermatt F (2023) The significance of partial migration for food web and ecosystem dynamics. Ecol Lett 26:3–22

Pulido F (2011) Evolutionary genetics of partial migration — the threshold model of migration revis(it)ed. Oikos 120: 1776–1783

Reis-Santos P, Tanner SE, Elsdon TS, Cabral HN, Gillanders BM (2013) Effects of temperature, salinity and water composition on otolith elemental incorporation of *Dicentrarchus labrax*. J Exp Mar Biol Ecol 446:245–252

Rikardsen AH, Elliott JM (2000) Variations in juvenile growth, energy allocation and life-history strategies of two populations of Arctic charr in North Norway. J Fish Biol 56:328–346

Rousseeuw PJ (1987) Silhouettes: a graphical aid to the interpretation and validation of cluster analysis. J Comput Appl Math 20:53–65

Sadovy Y, Severin KP (1992) Trace elements in biogenic aragonite: correlation of body growth rate and strontium levels in the otoliths of the white grunt, *Haemulon plumieri* (Pisces: Haemulidae). Bull Mar Sci 50:237–257

Sardá-Espinosa A (2019) Time-series clustering in R using the dtwclust package. R J 11:22–43

Schindler DE, Hilborn R, Chasco B, Boatright CP, Quinn TP, Rogers LA, Webster MS (2010) Population diversity and the portfolio effect in an exploited species. Nature 465: 609–612

Secor DH (2000) Spawning in the nick of time? Effect of adult demographics on spawning behaviour and recruitment in Chesapeake Bay striped bass. ICES J Mar Sci 57: 403–411

Secor DH (2015) Migration ecology of marine fishes. Johns Hopkins University Press, Baltimore, MD

Secor DH, Dean JM (1989) Somatic growth effects on the otolith–fish size relationship in young pond-reared striped bass, *Morone saxatilis*. Can J Fish Aquat Sci 46: 113–121

Secor DH, Houde ED (1995) Temperature effects on the timing of striped bass egg production, larval viability, and

recruitment potential in the Patuxent River (Chesapeake Bay). Estuaries 18:527–544

Secor DH, Piccoli PM (2007) Oceanic migration rates of Upper Chesapeake Bay striped bass (*Morone saxatilis*), determined by otolith microchemical analysis. Fish Bull 105:62–73

Secor DH, Dean JM, Laban EH (1991) Manual for otolith removal and preparation for microstructural examination. Belle W Baruch and Electric Power Research Institute, Columbia, SC

Secor DH, O'Brien MHP, Gahagan BI, Fox DA, Higgs AL, Best JE (2020) Multiple spawning run contingents and population consequences in migratory striped bass *Morone saxatilis.* PLOS ONE 15:e0242797

Seekell DA, Pace ML (2011) Climate change drives warming in the Hudson River Estuary, New York (USA). J Environ Monit 13:2321–2327

Sirois DL, Fredrick SW (1978) Phytoplankton and primary production in the lower Hudson River Estuary. Estuar Coast Shelf Sci 7:413–423

Stier AC, Shelton AO, Samhouri JF, Feist BE, Levin PS (2020) Fishing, environment, and the erosion of a population portfolio. Ecosphere 11:e03283

Sturrock AM, Hunter E, Milton JA, EIMF, Johnson RC, Waring CP, Trueman CN (2015) Quantifying physiological influences on otolith microchemistry. Methods Ecol Evol 6:806–816

Vanalderweireldt L, Winkler G, Mingelbier M, Sirois P (2019) Early growth, mortality, and partial migration of striped bass (*Morone saxatilis*) larvae and juveniles in the St. Lawrence estuary, Canada. ICES J Mar Sci 76: 2235–2246

Venables WN, Ripley BD (2002) Modern applied statistics with S, 4th edn. Springer, New York, NY

Volk EC, Blakley A, Schroder SL, Kuehner SM (2000) Otolith chemistry reflects migratory characteristics of Pacific salmonids: using otolith core chemistry to distinguish maternal associations with sea and freshwaters. Fish Res 46:251–266

Waldman JR, Grossfield J, Wirgin I (1988) Review of stock discrimination techniques for striped bass. N Am J Fish Manag 8:410–425

Walther BD (2019) The art of otolith chemistry: interpreting patterns by integrating perspectives. Mar Freshw Res 70: 1643

Walther BD, Limburg KE (2012) The use of otolith chemistry to characterize diadromous migrations. J Fish Biol 81: 796–825

Walther BD, Kingsford MJ, O'Callaghan MD, McCulloch MT (2010) Interactive effects of ontogeny, food ration and temperature on elemental incorporation in otoliths of a coral reef fish. Environ Biol Fishes 89:441–451

Wood SN (2017) Generalized additive models: an introduction with R, 2nd edn. Chapman & Hall/CRC, Boca Raton, FL

Wright MN, Ziegler A (2017) Ranger: a fast implementation of random forests for high dimensional data in C++ and R. J Stat Soft 77(1):1–17

Zlokovitz ER, Secor DH, Piccoli PM (2003) Patterns of migration in Hudson River striped bass as determined by otolith microchemistry. Fish Res 63:245–259

Editorial responsibility: Jana Davis, Annapolis, Maryland, USA
Reviewed by: T. R. Nelson, O. Morissette and 1 anonomous referee

Submitted: August 1, 2023
Accepted: February 5, 2024
Proofs received from author(s): March 16, 2024